225

Pattern formation in weakly damped parametric surface waves driven by two frequency components

By WENBIN ZHANG[1] AND JORGE VIÑALS[2]

[1]Department of Chemical Engineering, Massachusetts Institute of Technology, Cambridge, MA 02139, USA

[2]Supercomputer Computations Research Institute, Florida State University, Tallahassee, FL 32306-4052, USA, and Department of Chemical Engineering, FAMU-FSU College of Engineering, Tallahassee, FL 31310-6046, USA

A quasi-potential approximation to the Navier–Stokes equation for low-viscosity fluids is developed to study pattern formation in parametric surface waves driven by a force that has two frequency components. A bicritical line separating regions of instability to either of the driving frequencies is explicitly obtained, and compared with experiments involving a frequency ratio of 1/2. The procedure for deriving standing wave amplitude equations valid near onset is outlined for an arbitrary frequency ratio following a multiscale asymptotic expansion of the quasi-potential equations. Explicit results are presented for subharmonic response to a driving force of frequency ratio 1/2, and used to study pattern selection. Even though quadratic terms are prohibited in this case, hexagonal or triangular patterns are found to be stable in a relatively large parameter region, in qualitative agreement with experimental results.

1. Introduction

When a fluid layer is periodically oscillated in the direction normal to the free surface at rest, parametric surface waves (or Faraday waves) appear above a certain critical value of the vibration amplitude (Miles & Henderson 1990; Cross & Hohenberg 1993). We present in this paper an extension of a weakly nonlinear model previously introduced by Zhang & Viñals (1996, 1997), which is valid in the limit of low fluid viscosity, large aspect ratio and large depth, to study pattern selection near onset of Faraday waves when the driving force has two independent frequency components.

The model developed by Zhang & Viñals (1997) was based on a quasi-potential approximation to the equations governing fluid motion. In it, the flow is considered to be potential in the bulk, subject to effective boundary conditions at the moving free surface that incorporate the effect of the rotational component of the flow within a thin boundary layer near the free surface. We further assumed without rigorous justification that for low-viscosity fluids, only linear viscous terms need to be retained in the resulting equations (the so-called linear damping quasi-potential equations, or LDQPEs). A multiscale analysis of the resulting LDQPEs led to the prediction of standing wave patterns of square symmetry near onset for capillary waves, in agreement with experiments. For mixed capillary–gravity waves, patterns

of hexagonal symmetry or quasi-periodic patterns were predicted depending on the value of the damping coefficient.

Although some of our predictions have been confirmed experimentally (Kudrolli & Gollub 1996), we address in this paper pattern selection in systems driven by periodic forces comprising two frequency components for two reasons. First, recent detailed experiments involving two frequencies provide a good opportunity for additional tests of our theory. Second, additional control parameters appear relative to the single frequency case, namely the frequency ratio, relative amplitude and phase difference. Therefore, one may anticipate richer dynamics and more interesting steady states as compared to the single frequency case.

Consider a fluid layer perpendicular to the z-axis, driven by a force of the form

$$g_z(t) = -g_0 - g_z[r \sin 2m\omega_0 t + (1-r)\sin(2n\omega_0 t + \phi)], \tag{1.1}$$

where r ($0 \leqslant r \leqslant 1$) is the relative amplitude of the two frequency components, ϕ is their relative phase difference, g_0 is the constant background gravitational field pointing in the negative z-direction, and g_z is the amplitude of the oscillatory component. When r is sufficiently small, the forcing component $\sin(2n\omega_0 t + \phi)$ is expected to dominate, the other component ($\sin 2m\omega_0 t$) being a small perturbation. Linear stability of the flat surface is thus approximately determined by subharmonic instability to the forcing component $\sin(2n\omega_0 t + \phi)$ (note that this is not necessarily a subharmonic response to the entire driving force), with a critical wavenumber k_{0n} given by $g_0 k_{0n} + \Gamma k_{0n}^3/\rho = n^2\omega_0^2$, where Γ is the surface tension of the surface and ρ is the density of the fluid. On the other hand, when r is sufficiently close to 1, the forcing component $\sin 2m\omega_0 t$ dominates, and linear stability is approximately determined by subharmonic instability at a frequency $m\omega_0$ (again it is not necessary that it be a subharmonic response to the entire driving force), with a critical wavenumber k_{0m} given by $g_0 k_{0m} + \Gamma k_{0m}^3/\rho = m^2\omega_0^2$. When r is varied from 0 to 1, one could imagine that the above two instabilities can have the same threshold value of the driving amplitude g_z for some value of r, which will be referred to as the *bicritical* value r_b. Furthermore, given a fixed frequency ratio m/n, the bicritical value r_b can be a function of the phase difference ϕ. In the (r, ϕ)-plane, the bicritical values $r_b(\phi)$ form a line (the *bicritical line*) which separates the two regions with different characteristic temporal dependencies and spatial scales.

The first two-frequency Faraday experiments were reported by Edwards & Fauve (1992, 1993, 1994), albeit in fluids of large viscosity. In that case, and with a purely sinusoidal parametric force, roll patterns (or lines) similar to those observed in Rayleigh–Bénard convection are observed near the primary instability of a flat surface. In the case of two frequencies, Edwards & Fauve studied several ratios m/n, including 3/5, 4/5, 4/7, 6/7, and 8/9, with most of their data for the case $m/n = 4/5$. In this latter case, parametric surface waves were found to respond synchronously (harmonically) with the force when the even-frequency forcing component $\sin(2 \times 4\omega_0 t)$ dominates, and subharmonically when the odd-frequency forcing component $\sin(2 \times 5\omega_0 t + \phi)$ dominates. The bicritical line obtained by Edwards & Fauve is almost independent of the phase difference ϕ, and for $m/n = 4/5$, $r_b(\phi) \approx 0.32$.

They also found many interesting standing wave patterns near the primary instability of a planar surface: lines, squares, hexagons, and twelve-fold quasi-crystalline patterns. For the cases of $m/n = $ even/odd (4/5, 4/7, 6/7, and 8/9), hexagonal patterns were observed for a wide range of values of r, in the region of harmonic response in the (r, ϕ)-plane (when the even-frequency forcing component dominates).

On the same side of the bicritical line where hexagonal patterns are found, a stable twelve-fold quasi-crystalline pattern was observed in a small region very close to the bicritical line. For $m/n = 4/5$, this small region is around $r \approx 0.32$ and $\phi \approx 7.5°$.†

Two-frequency driven Faraday experiments using less-viscous fluids have been reported more recently by Müller (1993). In the case of single-frequency forcing, Müller observed standing wave patterns of square symmetry near onset, in agreement with previous experiments (Lang 1992; Ezerskii *et al.* 1986; Tufillaro & Gollub 1989; Ciliberto, Douady & Fauve 1991; Christiansen, Alstrøm & Levinsen 1992; Bosch & van de Water 1993; Edwards & Fauve 1993) and with our previous theoretical work (Zhang & Viñals 1997) for weak viscous dissipation. He also studied pattern formation near onset in a system driven by a two-frequency force, with frequency ratio $m/n = 1/2$, and found that the (r, φ)-plane is divided into two regions: in the region of larger r, parametric surface waves are found to respond subharmonically to the entire driving force, whereas in the region of smaller r surface waves respond harmonically. The bicritical line has an interesting dependence on the phase difference φ (in his notation), which was not observed by Edwards & Fauve (1993, 1994) for frequency ratios other than $1/2$ in highly viscous fluids.

In addition to square patterns, Müller found hexagonal patterns that respond harmonically to the driving force, and hexagonal or triangular patterns that respond subharmonically to the driving force. Interestingly, a spatially disordered region, that responds subharmonically to the driving force with an additional slow time dependence, was also found near onset.

We study in this paper how much of this seemingly complicated stability diagram found by Müller can be understood, at least qualitatively, in terms of perturbative analysis of the quasi-potential equations introduced by Zhang & Viñals (1996, 1997). In Müller's experiments, the damping parameter $\gamma = 2vk^2$, (where v is the kinematic viscosity of the fluid, and k the wavenumber of a surface Fourier mode) has the value $\gamma_s = 0.17$ in the region of subharmonic response, and $\gamma_h = 0.33$ in the region of harmonic response. Since the quasi-potential approximation is only valid in the limit of small viscous dissipation (small γ), we anticipate qualitative agreement with experiments, while smaller damping parameters are needed to quantitatively test our theoretical predictions.

The rest of this paper is organized as follows. In §2, we present analytical results for the bicritical lines, and make comparison with Müller's experimental results. Section 3 contains the derivation of standing wave amplitude equations (SWAEs), and results of pattern selection based on the SWAEs. Further discussion and conclusion are presented in §4.

2. Bicritical line

In this section, we consider the linear stability of two-frequency forced Faraday waves, and obtain analytical results for the bicritical line $r_b(\phi)$. We restrict our attention to cases in which m and n are two small positive integers that are relatively

† In the form of the driving force used by Edwards & Fauve, $-g_0 + a_0[\cos\chi\cos(4\omega t) + \sin\chi\cos(5\omega t + \phi')]$, the twelve-fold quasi-crystalline pattern was observed around $\chi \approx 65°$ and $\phi' \approx 75°$. Also, for later reference, we note that Müller (1993) used the definition $g(t) = -g_0 + g_z[r\cos 2\omega_0 t + (1-r)\cos(4\omega_0 t + \varphi)]$, which can be written in the form of (1.1) by the transformation of $t \to t + \pi/(4\omega_0)$ and $\varphi = \phi - \pi/2$.

prime (e.g, $m/n = 1/2, 1/3, 2/3$). Without loss of generality, we assume $m < n$. The phase difference ϕ can be chosen within $-\pi/m \leqslant \phi < \pi/m$ because $g(t)$ is invariant with respect to the transformation: $\phi \to \phi + 2\pi/m$ and $t \to t + j\pi/m\omega_0$ for any integer j that makes $(nj + 1)/m$ an integer. Linear stability of the free surface of a weakly viscous fluid of infinite depth under a two-frequency parametric force is determined by the damped Mathieu equation (Landau & Lifshitz 1976),

$$\partial_{tt}\hat{h}_k + 4\nu k^2 \partial_t \hat{h}_k + \left[g_0 k + \frac{\Gamma k^3}{\rho} + g_z k \left(r \sin 2m\omega_0 t + (1-r)\sin(2n\omega_0 t + \phi) \right) \right] \hat{h}_k = 0. \quad (2.1)$$

2.1. *Subharmonic versus synchronous responses*

The two-frequency parametric force in (2.1) has an angular frequency $2\omega_0$, or a period π/ω_0 (recall that m and n are assumed to be relatively prime). Whether a region is subharmonic or synchronous (harmonic) with respect to the total driving force depends on whether m/n is odd/odd, even/odd, or odd/even. This overall response to the total force is important since it can be easily determined experimentally by using stroboscopic methods. According to Floquet's theorem, the general form of the solutions of (2.1) is a periodic function multiplied by an exponential function of time. At the stability boundaries, (2.1) has periodic solutions, $\hat{h}_k(t + \pi/\omega_0) = p\hat{h}_k(t)$, where the Floquet multiplier $p = \pm 1$. For $p = -1$, $\hat{h}_k(t)$ has a period of $2\pi/\omega_0$, and thus the response is subharmonic, whereas for $p = 1$, $\hat{h}_k(t)$ has a period of π/ω_0, and hence the response is harmonic. Therefore the solution of (2.1) at the boundaries for subharmonic instability ($p = -1$) can be written as a Fourier series in odd frequencies $(2j - 1)\omega_0, j = 1, 2, \ldots, \infty$, whereas at the boundaries for harmonic instability ($p = 1$) the frequencies involved in the series are $2j\omega_0, j = 1, 2, \ldots, \infty$. As a consequence, when the odd (even) frequency dominates, the response is subharmonic (harmonic).

We now turn to a detailed calculation of the bicritical line in the (r, ϕ)-plane, starting from the linearized quasi-potential equation (2.1) (Zhang & Vinals 1996, 1997). Since the characteristic time and length scales are different on the two sides of the bicritical line for two-frequency driven Faraday waves, we shall use dimensional variables, and group them into dimensionless quantities when necessary. In order to keep our notation simple, we define $\delta = g_0 k + \Gamma k^3/\rho$, and $f = g_z k/4$. Equation (2.1) can now be written as

$$\partial_{tt}\hat{h}_k + 2\gamma\partial_t\hat{h}_k + [\delta + 4f(r\sin 2m\omega_0 t + (1-r)\sin(2n\omega_0 t + \phi))]\hat{h}_k = 0. \quad (2.2)$$

2.2. *Multiple-scale expansion*

We consider small values of the driving amplitude f and of the damping coefficient γ, and introduce a small parameter η such that $\gamma = \eta\gamma_0$ and $f = \eta f_0$. For simplicity, we will consider the wavenumber k_0 exactly at subharmonic resonance with either of the forcing components, and thus no expansion for the wavenumber is needed. Define $\delta_0 = g_0 k_0 + \Gamma k_0^3/\rho$, and seek a solution $\hat{h}_k$ in a power series in η as

$$\hat{h}_k = \hat{h}_k^{(0)}(t, T_1, T_2) + \eta\hat{h}_k^{(1)}(t, T_1, T_2) + \eta^2\hat{h}_k^{(2)}(t, T_1, T_2) + \cdots, \quad (2.3)$$

where $T_1 = \eta t$ and $T_2 = \eta^2 t$. We have introduced a second slow time scale T_2 in the expansion for $\hat{h}_k$, in addition to the slow time scale T_1. The second slow time scale is necessary since we are going to perform our perturbation expansion up to

$O(\eta^2)$, which is one order higher in η than the perturbation expansion for the case of a single sinusoidal driving force in Zhang & Vinals (1997).

Equation (2.2) contains a damping term proportional to γ, while terms of $O(\gamma^{3/2})$ and $O(\gamma^2)$ (or $O(\eta^2)$) have been neglected in the quasi-potential approximation (Zhang & Viñals 1997). It seems to be inconsistent to consider terms of $O(\eta^2)$ in the solutions to (2.2). The basic reason to consider solutions up to $O(\eta^2)$ here is that, as we shall see below, these terms can have relatively large coefficients due to the special nature of the expansion. When the dominant driving frequency is $2m\omega_0$, the small parameter in this perturbation expansion is the dimensionless driving amplitude $rf/(m^2\omega_0^2) \ll 1$. The driving force in this case can be written as

$$\frac{4rf}{m^2\omega_0^2} \left(\sin 2m\omega_0 t + \frac{1-r}{r} \sin(2n\omega_0 t + \phi) \right). \tag{2.4}$$

Since the perturbative expansion is in powers of $rf/(m^2\omega_0^2)$, as well as in $(1-r)/r$, it is necessary to assume that $(1-r)/r \sim O(1)$ or smaller. However, $(1-r)/r$ can be quite large on the bicritical line if $r = r_b(\phi)$ is small for some values of ϕ. In this case, higher-order terms in η can be important if they have factors of $(1-r)/r$ in their coefficients. In Müller's experiments, for example, the smallest value of $r_b(\phi)$ is about 0.2, and thus $(1-r)/r \sim 4$. Similar arguments can be made when $2n\omega_0$ is the dominating driving frequency. In the case of Müller's experiments, the largest value of $r/(1-r)$ along the bicritical line is less than 0.5. A consistent calculation would require keeping terms of $O(\gamma^{3/2})$ or higher at the linear level of approximation in the surface variables (equation (2.2)), leading to a much more involved nonlinear analysis. However, the agreement that we find with Müller's bicritical line is quite reasonable.

On substituting the expansion for $\hat{h}_k$ into (2.2), we have at $O(\eta^0)$

$$\partial_{tt}\hat{h}_k^{(0)} + \delta_0\hat{h}_k^{(0)} = 0. \tag{2.5}$$

At $O(\eta)$, we have

$$\partial_{tt}\hat{h}_k^{(1)} + \delta_0\hat{h}_k^{(1)} = -2\frac{\partial^2\hat{h}_k^{(0)}}{\partial T_1\partial t} - 2\gamma_0\frac{\partial\hat{h}_k^{(0)}}{\partial t} - 4f_0\left(r\sin 2m\omega_0 t + (1-r)\sin(2n\omega_0 t + \phi)\right)\hat{h}_k^{(0)}, \tag{2.6}$$

and at $O(\eta^2)$, we have

$$\partial_{tt}\hat{h}_k^{(2)} + \delta_0\hat{h}_k^{(2)} = -2\frac{\partial^2\hat{h}_k^{(0)}}{\partial T_2\partial t} - \frac{\partial^2\hat{h}_k^{(0)}}{\partial T_1^2} - 2\gamma_0\frac{\partial\hat{h}_k^{(0)}}{\partial T_1} - 2\frac{\partial^2\hat{h}_k^{(1)}}{\partial T_1\partial t} - 2\gamma_0\frac{\partial\hat{h}_k^{(1)}}{\partial t}$$
$$-4f_0\left(r\sin 2m\omega_0 t + (1-r)\sin(2n\omega_0 t + \phi)\right)\hat{h}_k^{(1)}. \tag{2.7}$$

We now consider separately the two cases of $\delta_0 = m^2\omega_0^2$ and $\delta_0 = n^2\omega_0^2$.

2.2.1. $\delta_0 = m^2\omega_0^2$

At $O(\eta^0)$, we have the solution $\hat{h}_k^{(0)} = A(T_1, T_2)\cos m\omega_0 t + B(T_1, T_2)\sin m\omega_0 t$. At $O(\eta)$, we have the following solvability condition in order to avoid secular terms:

$$\frac{\partial A}{\partial T_1} = \left(\frac{rf_0}{m\omega_0} - \gamma_0\right)A, \tag{2.8}$$

$$\frac{\partial B}{\partial T_1} = -\left(\frac{rf_0}{m\omega_0} + \gamma_0\right)B. \tag{2.9}$$

The solution at this order is

$$\hat{h}_k^{(1)} = -\frac{rf_0}{4m^2\omega_0^2}\left(B\cos 3m\omega_0 t - A\sin 3m\omega_0 t\right)$$

$$+\frac{(1-r)f_0}{2n(n-m)\omega_0^2}\left[B\cos\left((2n-m)\omega_0 t + \phi\right) + A\sin\left((2n-m)\omega_0 t + \phi\right)\right]$$

$$-\frac{(1-r)f_0}{2n(m+n)\omega_0^2}\left(B\cos\left((2n+m)\omega_0 t + \phi\right) - A\sin\left((2n+m)\omega_0 t + \phi\right)\right]. \quad (2.10)$$

Whether higher-order contributions are important or negligible is not known at this point. Since we have found non-trivial equations for the amplitude A and B, and these equations give us a threshold value of the driving amplitude $f_0 = m\omega_0\gamma_0/r$ for the Faraday instability, one would guess that it is not necessary to consider higher-order contributions. However, as we show below, contributions at $O(\eta^2)$ are important to determine the bicritical line $r_b(\phi)$. Interestingly, and for a quite obvious reason to be also discussed below, contributions at $O(\eta^2)$ for the case of $m/n = 1/2$ are qualitatively different from the cases of any other frequency ratios.

At $O(\eta^2)$, we have

$$\partial_{tt}\hat{h}_k^{(2)} + m^2\omega_0^2\hat{h}_k^{(2)}$$

$$= \left[2m\omega_0\frac{\partial A}{\partial T_2} - \frac{\partial^2 B}{\partial T_1^2} - 2\gamma_0\frac{\partial B}{\partial T_1} - \frac{f_0^2}{\omega_0^2}\left(\frac{r^2}{2m^2} + \frac{2(1-r)^2}{n^2-m^2}\right)B\right]\sin m\omega_0 t$$

$$-\left[2m\omega_0\frac{\partial B}{\partial T_2} + \frac{\partial^2 A}{\partial T_1^2} + 2\gamma_0\frac{\partial A}{\partial T_1} + \frac{f_0^2}{\omega_0^2}\left(\frac{r^2}{2m^2} + \frac{2(1-r)^2}{n^2-m^2}\right)A\right]\cos m\omega_0 t$$

$$-\frac{2m^2-mn+n^2}{2nm^2(n-m)}\frac{r(1-r)f_0^2}{\omega_0^2}\left(A\cos[(2n-3m)\omega_0 t + \phi] - B\sin[(2n-3m)\omega_0 t + \phi]\right)$$

$$+\frac{2m^2+mn+n^2}{2nm^2(n+m)}\frac{r(1-r)f_0^2}{\omega_0^2}\left(A\cos[(2n+3m)\omega_0 t + \phi] + B\sin[(2n+3m)\omega_0 t + \phi]\right)$$

$$-\frac{2(n^2+mn-m^2)}{mn(n^2-m^2)}\frac{r(1-r)f_0^2}{\omega_0^2}\left(A\cos[(2n-m)\omega_0 t + \phi] + B\sin[(2n-m)\omega_0 t + \phi]\right)$$

$$+\frac{2(n^2-mn-m^2)}{mn(n^2-m^2)}\frac{r(1-r)f_0^2}{\omega_0^2}\left(A\cos[(2n+m)\omega_0 t + \phi] + B\sin[(2n+m)\omega_0 t + \phi]\right)$$

$$+\frac{(1-r)^2f_0^2}{n(n-m)\omega_0^2}\left(A\cos[(4n-m)\omega_0 t + 2\phi] - B\sin[(4n-m)\omega_0 t + 2\phi]\right)$$

$$+\frac{(1-r)^2f_0^2}{n(m+n)\omega_0^2}\left(A\cos[(4n+m)\omega_0 t + 2\phi] + B\sin[(4n+m)\omega_0 t + 2\phi]\right)$$

$$-\frac{3r^2f_0^2}{2m^2\omega_0^2}\left(A[\cos 3m\omega_0 t - \cos 5m\omega_0 t] - B[\sin 3m\omega_0 t + \sin 5m\omega_0 t]\right). \quad (2.11)$$

Terms on the right-hand side of (2.11) will contribute to the solvability condition only if their frequencies are $m\omega_0$. Thus, besides the first two terms, only the third term contributes to the solvability condition when $2n - 3m = m$, i.e. the frequency ratio $m/n = 1/2$ (note $n > m$ by assumption). Therefore the solvability conditions at $O(\eta^2)$ for frequency ratio $m/n = 1/2$ is different from that for all other frequency ratios.

For $m/n = 1/2$, the solvability conditions are

$$\frac{\partial A}{\partial T_2} = \frac{1}{2\omega_0}\left[\frac{f_0^2}{\omega_0^2}\left(\frac{3r^2}{2} + \frac{2(1-r)^2}{3} + r(1-r)\cos\phi\right) - \gamma_0^2\right]B - \frac{r(1-r)f_0^2}{2\omega_0^3}A\sin\phi, \quad (2.12)$$

$$\frac{\partial B}{\partial T_2} = -\frac{1}{2\omega_0}\left[\frac{f_0^2}{\omega_0^2}\left(\frac{3r^2}{2} + \frac{2(1-r)^2}{3} + r(1-r)\cos\phi\right) - \gamma_0^2\right]A + \frac{r(1-r)f_0^2}{2\omega_0^3}B\sin\phi. \quad (2.13)$$

For a frequency ratio $m/n \neq 1/2$, the solvability conditions are

$$\frac{\partial A}{\partial T_2} = \frac{1}{2m\omega_0}\left[\frac{f_0^2}{\omega_0^2}\left(\frac{3r^2}{2m^2} + \frac{2(1-r)^2}{n^2 - m^2}\right) - \gamma_0^2\right]B, \quad (2.14)$$

$$\frac{\partial B}{\partial T_2} = -\frac{1}{2m\omega_0}\left[\frac{f_0^2}{\omega_0^2}\left(\frac{3r^2}{2m^2} + \frac{2(1-r)^2}{n^2 - m^2}\right) - \gamma_0^2\right]A. \quad (2.15)$$

Since we have assumed that T_1 and T_2 are two independent slow time scales in $A(T_1, T_2)$, we have the following relation when the original time scale t is used as the temporal parameter for $A(t)$ and $B(t)$:

$$\partial_t A = \eta\frac{\partial A}{\partial T_1} + \eta^2\frac{\partial A}{\partial T_2}, \quad (2.16)$$

$$\partial_t B = \eta\frac{\partial B}{\partial T_1} + \eta^2\frac{\partial B}{\partial T_2}. \quad (2.17)$$

We now combine the solvability conditions at $O(\eta)$ and at $O(\eta^2)$ by using the above two relations, and write both equations in the original time units (also recall that $f = \eta f_0$ and $\gamma = \eta\gamma_0$). For a frequency ratio $m/n = 1/2$, we have

$$\partial_t A = \frac{1}{2\omega_0}\left[\frac{f^2}{\omega_0^2}\left(\frac{3r^2}{2} + \frac{2(1-r)^2}{3} - r(1-r)\cos\phi\right) - \gamma^2\right]B$$
$$+ \left(\frac{rf}{\omega_0} - \frac{r(1-r)f^2}{2\omega_0^3}\sin\phi - \gamma\right)A, \quad (2.18)$$

$$\partial_t B = -\frac{1}{2\omega_0}\left[\frac{f^2}{\omega_0^2}\left(\frac{3r^2}{2} + \frac{2(1-r)^2}{3} + r(1-r)\cos\phi\right) - \gamma^2\right]A$$
$$- \left(\frac{rf}{\omega_0} - \frac{r(1-r)f^2}{2\omega_0^3}\sin\phi + \gamma\right)B. \quad (2.19)$$

The eigenvalues of the above linear system determine the linear stability of the flat surface for subharmonic resonance. The condition for linear instability is that at least one eigenvalue has a positive real part. This condition is

$$\left(\frac{rf}{\omega_0^2}\right)^2 - \frac{1-r}{r}\left(\frac{rf}{\omega_0^2}\right)^3\sin\phi - \left(\frac{\gamma}{\omega_0}\right)^2$$
$$> \frac{1}{4}\left[\left(\frac{3}{2} + \frac{2}{3}\left(\frac{1-r}{r}\right)^2\right)\left(\frac{rf}{\omega_0^2}\right)^2 - \left(\frac{\gamma}{\omega_0}\right)^2\right]^2 - \left(\frac{1-r}{2r}\right)^2\left(\frac{rf}{\omega_0^2}\right)^4, \quad (2.20)$$

where we have grouped the dimensionless damping parameter (γ/ω_0) and forcing amplitude (rf/ω_0^2) together, which are actually the expansion parameters. The right-hand side of (2.20) is of higher order in γ/ω_0 or in rf/ω_0^2 than the left-hand side. However, as we shall see later $(1-r)/r \approx 4$ for certain values of ϕ along the

bicritical line; thus the first term on the right-hand side has a quite large coefficient: $37.0(rf/\omega_0^2)^4$. Because of that, we do not neglect higher-order terms on the right-hand side unless we consider the case of extremely weak damping $\gamma/\omega_0 \ll 0.16$. We have also checked that corrections to the threshold value of the driving force from orders higher than $O(\eta^2)$ do *not* contain terms of the form of $((1-r)/r)^n(rf/\omega_0^2)^n$ for $n > 4$. Therefore the truncation at $O(\eta^2)$ is a good approximation.

For frequency ratios $m/n \neq 1/2$, the instability condition is,

$$\left(\frac{rf}{m^2\omega_0^2}\right)^2 - \left(\frac{\gamma}{m\omega_0}\right)^2 > \frac{1}{4}\left[\frac{r^2f^2}{m^4\omega_0^4}\left(\frac{3}{2} + \frac{2m^2}{n^2-m^2}\left(\frac{1-r}{r}\right)^2\right) - \left(\frac{\gamma}{m\omega_0}\right)^2\right]^2. \quad (2.21)$$

2.2.2. $\delta_0 = n^2\omega_0^2$

In this case, the condition for the Faraday instability up to $O(\eta)$ is,

$$\frac{(1-r)f}{n\omega_0} > \gamma. \quad (2.22)$$

The instability condition up to $O(\eta^2)$ for the case of frequency ratio $m/n = 1/2$ is given by

$$\left(\frac{(1-r)f}{4\omega_0^2}\right) + \left(\frac{2r}{1-r}\right)^2\left(\frac{(1-r)f}{4\omega_0^2}\right)^3\sin\phi - \left(\frac{\gamma}{2\omega_0}\right)^2 + 4\left(\frac{r}{1-r}\right)^4\left(\frac{(1-r)f}{4\omega_0^2}\right)^4$$

$$> \frac{1}{4}\left[\left(\frac{3}{2} - \frac{2}{3}\left(\frac{2r}{1-r}\right)^2\right)\left(\frac{(1-r)f}{4\omega_0^2}\right)^2 - \left(\frac{\gamma}{2\omega_0}\right)^2\right]^2, \quad (2.23)$$

In this case, since $r/(1-r)$ is expected to be small (in Müller's experiment, $r/(1-r) < 0.45$) along the bicritical line, the approximate threshold value of the driving force f_{th} can be found with relatively good accuracy by solving (2.23) perturbatively:

$$\frac{(1-r)f_{th}}{4\omega_0^2} = \frac{\gamma}{2\omega_0} + b_1\left(\frac{\gamma}{2\omega_0}\right)^2 + b_2\left(\frac{\gamma}{2\omega_0}\right)^3 + \cdots, \quad (2.24)$$

where

$$b_1 = -2\left(\frac{r}{1-r}\right)^2\sin\phi, \quad (2.25)$$

$$b_2 = 10\left(\frac{r}{1-r}\right)^4\sin^2\phi + \frac{1}{2}\left[\frac{1}{4} - \frac{4}{3}\left(\frac{r}{1-r}\right)^2\right]^2 - 2\left(\frac{r}{1-r}\right)^4. \quad (2.26)$$

In terms of the driving amplitude g_z, the threshold value is

$$g_z^{12h} = \frac{16\nu k_{12h}\omega_0}{1-r}\left[1 + b_1\frac{\nu k_{12h}^2}{\omega_0} + b_2\left(\frac{\nu k_{12h}^2}{\omega_0}\right)^2\right], \quad (2.27)$$

where k_{12h} is determined by $g_0 k_{12h} + \Gamma k_{12h}^3/\rho = 4\omega_0^2$.

For frequency ratios where $m/n \neq 1/2$, the instability condition is

$$\left(\frac{(1-r)f}{n^2\omega_0^2}\right)^2 - \left(\frac{\gamma}{n\omega_0}\right)^2 > \frac{1}{4}\left[\frac{(1-r)^2f^2}{n^4\omega_0^4}\left(\frac{3}{2} - \frac{2n^2}{n^2-m^2}\left(\frac{r}{1-r}\right)^2\right) - \left(\frac{\gamma}{n\omega_0}\right)^2\right]^2.$$
$$(2.28)$$

The threshold value of the driving amplitude g_z is

$$g_z^{(n)} = \frac{8n\nu k_n \omega_0}{1-r}\left[1 + \frac{1}{8}\left(\frac{1}{2} - \frac{2n^2}{n^2-m^2}\left(\frac{r}{1-r}\right)^2\right)^2\left(\frac{2\nu k_n^2}{n\omega_0}\right)^2\right], \qquad (2.29)$$

where k_n is determined by $g_0 k_n + \Gamma k_n^3/\rho = n^2\omega_0^2$.

For a frequency ratio $m/n = 1/2$, subharmonic resonance and harmonic resonance will occur simultaneously (for the same value of the driving amplitude) when $g_z^{(12s)} = g_z^{(12h)}$. The value of $g_z^{(12s)}$ is given (2.20), which is written as follows:

$$f_s^2 - \frac{1-r}{r}f_s^3\sin\phi - \gamma_s^2 = \frac{1}{4}\left[\left(\frac{3}{2} + \frac{2}{3}\left(\frac{1-r}{r}\right)^2\right)f_s^2 - \gamma_s^2\right]^2 - \left(\frac{1-r}{2r}\right)^2 f_s^2, \quad (2.30)$$

where $f_s = rg_z^{(12s)}k_{12s}/(4\omega_0^2)$ and $\gamma_s = 2\nu k_{12s}^2/\omega_0$. The value of $g_z^{(12h)}$ is given by (2.23), which can be written as

$$f_h^2 + \left(\frac{2r}{1-r}\right)^2 f_h^3\sin\phi - \gamma_h^2 = \frac{1}{4}\left[\left(\frac{3}{2} - \frac{2}{3}\left(\frac{2r}{1-r}\right)^2\right)f_h^2 - \gamma_h^2\right]^2 - 4\left(\frac{rf_h}{1-r}\right)^4, \quad (2.31)$$

where $f_h = (1-r)g_z^{(12h)}k_{12h}/(16\omega_0^2)$ and $\gamma_h = \nu k_{12h}^2/\omega_0$. The bicritical line $r_b(\phi)$ can be obtained directly by solving (2.30) and (2.31) numerically. Alternatively, $r_b(\phi)$ can be obtained by substituting the expression for $g_z^{(12h)}$ of (2.27) as well as that of $g_z^{(12s)}$ into (2.30), and then solving (2.30). Except for a small difference near $\phi = \pi/2$, where r is largest on the bicritical line, the second way is much easier. In the results presented below, the values of $r_b(\phi)$ directly calculated from (2.30) and (2.31) are used.

The solid curve in figure 1 is the bicritical line calculated by using parameters appropriate for the experimental data of Müller (1993). Note that for simplicity we have considered surface waves in the infinite depth limit in the above calculations. By assuming that the viscous dissipation near the bottom boundary layer can be neglected, our results can be generalized to the case of a fluid layer of finite depth d by replacing the infinite-depth dispersion relation by $\omega(k)^2 = \tanh(kd)(g_0 k + \Gamma k^3/\rho)$ and g_z by $g_z\tanh(kd)$. Since $k_{12s}d = 2.0$ and $k_{12h}d = 3.9$ in Müller's experiments, such finite-depth corrections are small, but have been included in figure 1. We also note that the value of k_{12s} calculated from the finite-depth dispersion relation using appropriate fluid and forcing parameters is different from that observed experimentally by Müller, and we have used the experimental value of wavenumber k_{12s}†. Our analytical results agree qualitatively with the experimental results of Müller, shown as grey symbols. Other curves in figure 1 are bicritical lines for the same values of ω_0, k_{12s}, and k_{12h} as the solid curve, but $\nu = 0.15$ for the dotted curve, $\nu = 0.1$ for the dashed curve, and $\nu = 0.05$ for the long-dashed curve. Therefore our calculation is in qualitative agreement with the bicritical line determined experimentally. The small quantitative discrepancy between our analytical results and experimental results is probably due to the relatively large values of the damping parameters ($\gamma_s = 0.17$ and $\gamma_h = 0.33$). It is likely that the quasi-potential approximation is not accurate in this parameter range.

† The value of k_{12s} calculated from the finite-depth dispersion relation using appropriate fluid and forcing parameters ($\rho = 0.95 > $ g cm^3, $\Gamma = 20.6$ dyn cm^{-1}, $d = 0.23$ cm, and $\omega_0 = 2\pi \times 27.9$ Hz) is 10 cm^{-1}, or $\lambda_{12s} = 0.63$ cm. This value of the critical wavelength is significantly different from what was observed by Müller, $\lambda_{12s} \approx 0.72$ cm. The calculated value of k_{12h} does agree well with the observed value, $k_{12h} = 17$ cm^{-1}, or $\lambda_{12h} \approx 0.37$ cm.
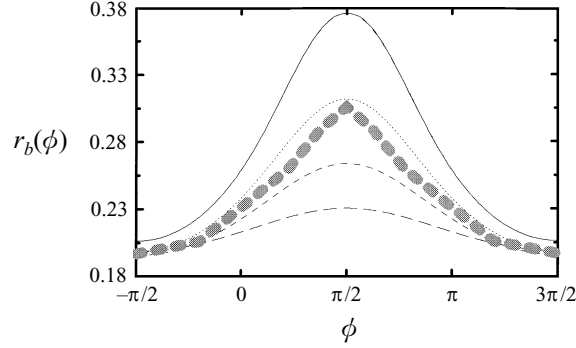
FIGURE 1. Bicritical lines of Faraday waves driven by a two-frequency force of frequency ratio $m/n = 1/2$. The grey symbols are taken from Müller's experiment (Müller 1993), and the solid curve is calculated using parameters of Müller's experiment: $v = 0.2$ cm^2 s^{-1}, $\omega_0/2\pi = 27.9$ Hz, $k_{12s} = 8.7$ cm^{-1}, and $k_{12h} = 17.0$ cm^{-1}. Other curves are calculated using the same values of ω_0, k_{12s}, and k_{12h} as the solid curve, but $v = 0.15$ cm^2 s^{-2} for the dotted curve, $v = 0.1$ cm^2 s^{-2} for the dashed curve, and $v = 0.05$ cm^2 s^{-2} for the long-dashed curve.

For frequency ratios $m/n \neq 1/2$, we predict that the bicritical line is independent of the phase difference ϕ, and can be readily obtained from (2.21) and (2.28). Further experimental studies of bicritical lines for different values of frequency ratio, v, ω_0, and surface tension Γ would be interesting to provide additional tests of our results.

3. Standing wave amplitude equations

We present in this section a weakly nonlinear analysis of parametric surface waves driven by two frequencies, extending the calculations presented earlier for the single-frequency case by Zhang & Vinals (1997). For fluids of low viscosity, the equations governing fluid flow and the boundary conditions at the free surface were expanded in the (small) width of the vortical layer adjacent to the free surface. The bulk flow is then potential, but satisfies effective boundary conditions on the moving surface. We furthermore neglected viscous terms that are nonlinear in the free surface variables to arrive at the so-called linear damping quasi-potential equations. They involve only the surface's deviation away from planarity h, and the surface velocity potential Φ, but no longer depend on the bulk velocity field

$$\partial_t h(\boldsymbol{x}, t) = \gamma \nabla^2 h + \hat{\mathscr{D}} \Phi - \nabla \cdot (h \nabla \Phi) + \tfrac{1}{2} \nabla^2 (h^2 \hat{\mathscr{D}} \Phi)$$
$$- \hat{\mathscr{D}}(h \hat{\mathscr{D}} \Phi) + \hat{\mathscr{D}} \left[h \hat{\mathscr{D}}(h \hat{\mathscr{D}} \Phi) + \tfrac{1}{2} h^2 \nabla^2 \Phi \right], \tag{3.1}$$

$$\partial_t \Phi(\boldsymbol{x}, t) = \gamma \nabla^2 \Phi - (G_0 - \Gamma_0 \nabla^2) h - 4f (\sin 2t + \kappa \sin(2pt + \Theta)) h$$
$$+ \tfrac{1}{2} \left(\hat{\mathscr{D}} \Phi \right)^2 - \tfrac{1}{2} (\nabla \Phi)^2 - (\hat{\mathscr{D}} \Phi) \left[h \nabla^2 \Phi + \hat{\mathscr{D}}(h \hat{\mathscr{D}} \Phi) \right] - \tfrac{1}{2} \Gamma_0 \nabla \cdot \left(\nabla h (\nabla h)^2 \right). \tag{3.2}$$

Linearization of these two equations leads to (2.2). When the forcing component $\sin 2m\omega_0 t$ dominates, we choose $1/(m\omega_0)$ as the unit of time and $1/k_{0m}$ as the unit of length with $g_0 k_{0m} + \Gamma k_{0m}^3/\rho = m^2 \omega_0^2$. For the other case when the forcing component $\sin 2n\omega_0 t$ dominates, we choose $1/(n\omega_0)$ as the unit of time and $1/k_{0n}$ as the unit of length with $g_0 k_{0n} + \Gamma k_{0n}^3/\rho = n^2 \omega_0^2$. $\hat{\mathscr{D}}$ is a linear and non-local operator that multiplies each Fourier component of a field by its wavenumber modulus (Zhang & Viñals 1997). We can write the system of equations for the two cases in the same

dimensionless form, with the dimensionless variables γ, G_0, Γ_0, f, κ, and p having different values for the two cases. When the forcing component $\sin 2m\omega_0 t$ dominates, we have

$$\gamma = \frac{2\nu k_{0m}^2}{m\omega_0}, \quad f = \frac{g_z k_{0m} r}{4m^2\omega_0^2}, \quad \kappa = \frac{1-r}{r}, \quad p = \frac{n}{m}, \tag{3.3}$$

$$G_0 = \frac{g_0 k_{0m}}{m^2\omega_0^2}, \quad \Gamma_0 = \frac{\Gamma k_{0m}^3}{\rho m^2\omega_0^2} \quad (G_0 + \Gamma_0 = 1), \quad \Theta = \phi. \tag{3.4}$$

For the other case (the forcing component $\sin 2n\omega_0 t$ dominates), we have

$$\gamma = \frac{2\nu k_{0n}^2}{n\omega_0}, \quad f = \frac{g_z k_{0n}(1-r)}{4n^2\omega_0^2}, \quad \kappa = \frac{r}{1-r}, \quad p = \frac{m}{n}, \tag{3.5}$$

$$G_0 = \frac{g_0 k_{0n}}{n^2\omega_0^2}, \quad \Gamma_0 = \frac{\Gamma k_{0n}^3}{\rho n^2\omega_0^2} \quad (G_0 + \Gamma_0 = 1), \quad \Theta = -\frac{m}{n}\phi. \tag{3.6}$$

3.1. *Derivation of SWAEs*

As mentioned above, the detailed procedure for the derivation of standing wave amplitude equations parallels that presented by Zhang & Vinals (1997) for the case of sinusoidal forcing. We seek nonlinear standing wave solutions of Faraday waves near onset, i.e. $\varepsilon = (f - \gamma)/\gamma \ll 1$. The quasi-potential equations (Eqs. (3.1) and (3.2)) are expanded consistently in $\varepsilon^{1/2}$ with multiple time scales,

$$h(x, t, T) = \varepsilon^{1/2} h_1(x, t, T) + \varepsilon h_2 + \varepsilon^{3/2} h_3 + \cdots, \tag{3.7}$$

$$\Phi(x, t, T) = \varepsilon^{1/2} \Phi_1(x, t, T) + \varepsilon \Phi_2 + \varepsilon^{3/2} \Phi_3 + \cdots, \tag{3.8}$$

where h_1 and Φ_1 are the linear neutral solutions and can be found in a similar way to the case of sinusoidal forcing. For simplicity, we shall only consider terms up to order f or γ for h_1 and Φ_1. They are

$$h_1(x, t) = \left[\cos t + \frac{\gamma}{4}\sin 3t + \frac{\gamma\kappa}{2p(p+1)}\sin((2p+1)t + \Theta) \right.$$

$$\left. + \frac{\gamma\kappa}{2p(p-1)}\sin((2p-1)t + \Theta) \right] \sum_{j=1}^{N}\left[A_j(T)\exp\left(\hat{k}_j \cdot x\right) + \text{c.c.} \right], \tag{3.9}$$

$$\Phi_1(x, t) = \left[-\sin t + \gamma\cos t + \frac{3\gamma}{4}\cos 3t + \frac{\gamma\kappa(2p+1)}{2p(p+1)}\cos((2p+1)t + \Theta) \right.$$

$$\left. + \frac{\gamma\kappa(2p-1)}{2p(p-1)}\cos((2p-1)t + \Theta) \right] \sum_{j=1}^{N}\left[A_j(T)\exp\left(\hat{k}_j \cdot x\right) + \text{c.c.} \right], \tag{3.10}$$

where $T = \varepsilon t$.

At $O(\varepsilon)$, we have the following non-homogeneous linear equation for h_2:

$$\partial_{tt}h_2 - 2\gamma\nabla^2\partial_t h_2 + (G_0 - \Gamma_0\nabla^2)\hat{\mathscr{D}}h_2 + 4\gamma\left(\sin 2t + \kappa\sin(2pt + \Theta)\right)\hat{\mathscr{D}}h_2$$

$$= \sum_{j,l=1}^{N}\left\{ \frac{1+c_{jl}}{4}[2(1+c_{jl})]^{1/2} - \cos 2t\left[1 + c_{jl} - \frac{3-c_{jl}}{4}[2(1+c_{jl})]^{1/2} \right] \right.$$

$$\left. -\gamma\sin 2t\left[(5/2 + c_{jl})\left(1 + c_{jl} - [2(1+c_{jl})]^{1/2}\right) + \frac{1+c_{jl}}{8}[2(1+c_{jl})]^{1/2} \right] \right.$$

$$+\frac{2\gamma\kappa}{1-p^2}\sin(2pt+\Theta)\left[\frac{1+c_{jl}}{4}[2(1+c_{jl})]^{1/2}+p^2\left(1+c_{jl}-[2(1+c_{jl})]^{1/2}\right)\right]$$

$$-\frac{\gamma\kappa}{p}\sin[2(p+1)t+\Theta]\left[\frac{2p+1}{p+1}(1+c_{jl})[2(1+c_{jl})]^{1/2}+(p+1)\left(1+c_{jl}-[2(1+c_{jl})]^{1/2}\right)\right]$$

$$+\frac{\gamma\kappa}{p}\sin[2(p-1)t+\Theta]\left[\frac{2p-1}{p-1}(1+c_{jl})[2(1+c_{jl})]^{1/2}+(p-1)\left(1+c_{jl}-[2(1+c_{jl})]^{1/2}\right)\right]\Bigg\}$$

$$\times\left[A_jA_l\exp\left(i(\hat{\boldsymbol{k}}_j+\hat{\boldsymbol{k}}_l)\cdot\boldsymbol{x}\right)+\text{c.c.}\right]$$

$$+\sum_{j,l=1}^{N}\Bigg\{\frac{1-c_{jl}}{4}[2(1-c_{jl})]^{1/2}-\cos 2t\left[1-c_{jl}-\frac{3+c_{jl}}{4}[2(1-c_{jl})]^{1/2}\right]$$

$$-\gamma\sin 2t\left[(5/2-c_{jl})\left(1-c_{jl}-[2(1-c_{jl})]^{1/2}\right)+\frac{1-c_{jl}}{8}[2(1-c_{jl})]^{1/2}\right]$$

$$+\frac{2\gamma\kappa}{1-p^2}\sin(2pt+\Theta)\left[\frac{1-c_{jl}}{4}[2(1-c_{jl})]^{1/2}+p^2\left(1-c_{jl}-[2(1-c_{jl})]^{1/2}\right)\right]$$

$$-\frac{\gamma\kappa}{p}\sin[2(p+1)t+\Theta]\left[\frac{2p+1}{p+1}(1-c_{jl})[2(1-c_{jl})]^{1/2}+(p+1)\left(1-c_{jl}-[2(1-c_{jl})]^{1/2}\right)\right]$$

$$+\frac{\gamma\kappa}{p}\sin[2(p-1)t+\Theta]\left[\frac{2p-1}{p-1}(1-c_{jl})[2(1-c_{jl})]^{1/2}+(p-1)\left(1-c_{jl}-[2(1-c_{jl})]^{1/2}\right)\right]\Bigg\}$$

$$\times\left[A_jA_l^*\exp\left(i(\hat{\boldsymbol{k}}_j-\hat{\boldsymbol{k}}_l)\cdot\boldsymbol{x}\right)+\text{c.c.}\right]. \tag{3.11}$$

Before obtaining the detailed form of the equations, let us mention that the generic form of the SWAEs for two-frequency driven Faraday waves can be obtained by symmetry considerations (Edwards & Fauve 1994). For the case of single-frequency forcing the SWAEs derived in Zhang & Vinals (1997) contain only third-order nonlinear terms, but no quadratic terms. The exclusion of quadratic terms can be understood there from the requirement of sign invariance of the SWAEs. Subharmonic response of the fluid surface to the driving force $f\sin(2\omega_0 t)$ implies $h_j(\boldsymbol{x},t+\pi/\omega_0)=-h_j(\boldsymbol{x},t)$. Here h_j is a linear unstable mode,

$$h_j=\left(\cos\omega_0 t+\tfrac{1}{4}f\sin 3\omega_0 t+\cdots\right)\left(A_j\exp\left(i\hat{\boldsymbol{k}}_j\cdot\boldsymbol{x}\right)+\text{c.c.}\right), \tag{3.12}$$

where only odd multiples of frequency ω_0 appear. As a result, a sign change of A_j is equivalent to a time displacement in a period of the driving force, $t\to t+\pi/\omega_0$. Because of the invariance of the surface wave system under such a time displacement, the amplitude equation of A_j must be sign invariant, which obviously excludes quadratic terms. However, quadratic terms can arise with two-frequency forcing. If the frequency ratio $m/n=$ even/odd or odd/even, the SWAEs are sign invariant if the odd frequency dominates, and otherwise if the even frequency dominates. When the frequency ratio $m/n=$ odd/odd, the SWAEs are sign invariant. A general consequence of the loss of sign invariance is the appearance of quadratic terms in the amplitude equation.

We concentrate here on the case of frequency ratio $m/n=1/2$, since detailed experimental results are available for this case. Similar calculations can be done for other frequency ratios, and they might be interesting for future experimental studies. We further restrict our attention to the case that the odd frequency dominates, which also corresponds to the subharmonic side of the bicritical line. In this case, the

solutions at $O(\varepsilon^{1/2})$ are

$$h_1 = \left[\cos t + \frac{\gamma}{4}\sin 3t + \frac{\gamma\kappa}{4}\sin(3t+\phi)\right]\sum_{j=1}^{N}\left[A_j\exp\left(\hat{\boldsymbol{k}}_j\cdot\boldsymbol{x}\right)+\text{c.c.}\right], \tag{3.13}$$

$$\Phi_1 = \left[-\sin t + \gamma\cos t + \frac{3\gamma}{4}\cos 3t + \frac{3\gamma\kappa}{4}\cos(3t+\phi)\right]\sum_{j=1}^{N}\left[A_j\exp\left(\hat{\boldsymbol{k}}_j\cdot\boldsymbol{x}\right)+\text{c.c.}\right], \tag{3.14}$$

where $\kappa = (1-r)/r$. At $O(\varepsilon)$, we have

$$\begin{aligned}
&\partial_{tt}h_2 - 2\gamma\nabla^2\partial_t h_2 + (G_0 - \Gamma_0\nabla^2)\hat{\mathscr{D}}h_2 + 4\gamma\left(\sin 2t + \kappa\sin(4t+\phi)\right)\hat{\mathscr{D}}h_2 \\
&= \sum_{j,l=1}^{N}\left\{\frac{1+c_{jl}}{4}[2(1+c_{jl})]^{1/2} - \cos 2t\left[1+c_{jl} - \frac{3-c_{jl}}{4}[2(1+c_{jl})]^{1/2}\right.\right. \\
&\quad\left. -\tfrac{1}{2}\gamma\kappa\sin\phi\left(1+c_jl+(2+3c_{jl})[2(1+c_{jl})]^{1/2}\right)\right] \\
&\quad -\gamma\sin 2t\left[(5/2+c_{jl})\left(1+c_{jl}-[2(1+c_{jl})]^{1/2}\right)+\frac{1+c_{jl}}{8}[2(1+c_{jl})]^{1/2}\right. \\
&\quad\left.\left. -\tfrac{1}{2}\kappa\cos\phi\left(1+c_jl+(2+3c_{jl})[2(1+c_{jl})]^{1/2}\right)\right]\right\}\left[A_jA_l\exp\left(\text{i}(\hat{\boldsymbol{k}}_j+\hat{\boldsymbol{k}}_l)\cdot\boldsymbol{x}\right)+\text{c.c.}\right] \\
&\quad +\sum_{j,l=1}^{N}\left\{\frac{1-c_{jl}}{4}[2(1-c_{jl})]^{1/2} - \cos 2t\left[1-c_{jl} - \frac{3+c_{jl}}{4}[2(1-c_{jl})]^{1/2}\right.\right. \\
&\quad\left. -\tfrac{1}{2}\gamma\kappa\sin\phi\left(1-c_{jl}+(2-3c_{jl})[2(1-c_{jl})]^{1/2}\right)\right] \\
&\quad -\gamma\sin 2t\left[(5/2-c_{jl})\left(1-c_{jl}-[2(1-c_{jl})]^{1/2}\right)+\frac{1-c_{jl}}{8}[2(1-c_{jl})]^{1/2}\right. \\
&\quad\left.\left. -\tfrac{1}{2}\kappa\cos\phi\left(1-c_{jl}+(2-3c_{jl})[2(1-c_{jl})]^{1/2}\right)\right]\right\}\left[A_jA_l^*\exp\left(\text{i}(\hat{\boldsymbol{k}}_j-\hat{\boldsymbol{k}}_l)\cdot\boldsymbol{x}\right)+\text{c.c.}\right].
\end{aligned} \tag{3.15}$$

We now solve (3.15) for h_2. Since there are no secular terms on the right-hand side, we are only interested in the particular solution for h_2 caused by the right-hand side of that equation. The particular solution is

$$\begin{aligned}
h_2 = \sum_{j,l=1}^{N}&\left\{\left(\alpha_{jl} + \beta_{jl}\cos 2t + \gamma\delta_{jl}\sin 2t\right)\left[A_jA_l\exp\left(\text{i}(\hat{\boldsymbol{k}}_j+\hat{\boldsymbol{k}}_l)\cdot\boldsymbol{x}\right)+\text{c.c.}\right]\right. \\
&\left. + \left(\bar{\alpha}_{jl} + \bar{\beta}_{jl}\cos 2t + \gamma\bar{\delta}_{jl}\sin 2t\right)\left[A_jA_l^*\exp\left(\text{i}(\hat{\boldsymbol{k}}_j-\hat{\boldsymbol{k}}_l)\cdot\boldsymbol{x}\right)+\text{c.c.}\right]\right\}, \tag{3.16}
\end{aligned}$$

where

$$\alpha_{jl} = \frac{1+c_{jl}}{4\left[G_0+2\Gamma_0(1+c_{jl})\right]} - \frac{2\gamma^2\delta_{jl}}{G_0+2\Gamma_0(1+c_{jl})}, \tag{3.17}$$

$$\beta_{jl} = \frac{-H_{jl}\left(E_{jl}-8\gamma^2 M_{jl}\right) + \gamma^2\left(8(1+c_{jl})-2\kappa[2(1+c_{jl})]^{1/2}\cos\phi\right)N_{jl}}{\gamma^2\left(8(1+c_{jl})-2\kappa[2(1+c_{jl})]^{1/2}\cos\phi\right)^2 + E_{jl}^2 - 8\gamma^2 E_{jl}M_{jl}}, \tag{3.18}$$

$$\delta_{jl} = -\frac{\left(8(1 + c_{jl}) - 2\kappa[2(1 + c_{jl})]^{1/2} \cos \phi\right) H_{jl} + E_{jl} N_{jl}}{\gamma^2 \left(8(1 + c_{jl}) - 2\kappa[2(1 + c_{jl})]^{1/2} \cos \phi\right)^2 + E_{jl}^2 - 8\gamma^2 E_{jl} M_{jl}},$$ (3.19)

$$M_{jl} = \frac{[2(1 + c_{jl})]^{1/2}}{G_0 + 2\Gamma_0(1 + c_{jl})},$$ (3.20)

$$D_{jl} = \left[G_0 + 2\Gamma_0(1 + c_{jl})\right] [2(1 + c_{jl})]^{1/2} - 4,$$ (3.21)

$$E_{jl} = D_{jl} + 2\kappa\gamma[2(1 + c_{jl})]^{1/2} \sin \phi,$$ (3.22)

$$H_{jl} = 1 + c_{jl} - \frac{3 - c_{jl}}{4}[2(1 + c_{jl})]^{1/2} - \tfrac{1}{2}\kappa\gamma \left(1 + c_{jl} + (2 + 3c_{jl})[2(1 + c_{jl})]^{1/2}\right) \sin \phi,$$ (3.23)

and

$$N_{jl} = \left(5/2 + c_{jl}\right) \left(1 + c_{jl} - [2(1 + c_{jl})]^{1/2}\right) + \frac{1 + c_{jl}}{8}[2(1 + c_{jl})]^{1/2} + (1 + c_{jl})M_{jl}$$

$$- \tfrac{1}{2}\kappa \left(1 + c_{jl} + (2 + 3c_{jl})[2(1 + c_{jl})]^{1/2}\right) \cos \phi.$$ (3.24)

$\bar{\alpha}_{jl}$, $\bar{\beta}_{jl}$, and $\bar{\delta}_{jl}$ can be obtained by replacing c_{jl} with $-c_{jl}$ in the expressions for α_{jl}, β_{jl}, and δ_{jl} respectively.

The solution for Φ_2 is

$$\Phi_2 = \sum_{j,l=1}^{N} \left\{ (\gamma u_{jl} + \gamma v_{jl} \cos 2t + w_{jl} \sin 2t) \left[A_j A_l \exp\left(i(\hat{\boldsymbol{k}}_j + \hat{\boldsymbol{k}}_l) \cdot \boldsymbol{x}\right) + \text{c.c.}\right] \right.$$

$$\left. + (\gamma \bar{u}_{jl} + \gamma \bar{v}_{jl} \cos 2t + \bar{w}_{jl} \sin 2t) \left[A_j A_l^* \exp\left(i(\hat{\boldsymbol{k}}_j - \hat{\boldsymbol{k}}_l) \cdot \boldsymbol{x}\right) + \text{c.c.}\right] \right\},$$ (3.25)

where

$$u_{jl} = \tfrac{1}{2} + \left(\alpha_{jl} - \tfrac{1}{4}\right) [2(1 + c_{jl})]^{1/2},$$ (3.26)

$$v_{jl} = \tfrac{3}{4} + \left(\beta_{jl} - \tfrac{3}{8}\right) [2(1 + c_{jl})]^{1/2} + \frac{2\delta_{jl}}{[2(1 + c_{jl})]^{1/2}},$$ (3.27)

$$w_{jl} = -\tfrac{1}{2} + \tfrac{1}{4}[2(1 + c_{jl})]^{1/2} - \frac{2\beta_{jl}}{[2(1 + c_{jl})]^{1/2}},$$ (3.28)

and $\bar{u}_{jl}$, $\bar{v}_{jl}$, and $\bar{w}_{jl}$ can be obtained by replacing c_{jl} with $-c_{jl}$ in the expressions for u_{jl}, v_{jl}, and w_{jl} respectively.

We note that the triad resonant condition is $E_{jl} = 0$ in (3.23), which is different from that of the case of sinusoidal forcing ($D_{jl} = 0$) (Zhang & Viñals 1997). This difference is important since it results in different values of c_{jl} at the triad resonance, which is now also a function of the damping parameter γ, the ratio of amplitudes r, and the phase difference ϕ. As an example, figure 2 shows the modified triad resonant condition for $\Gamma_0 = 1$, $\gamma = 0.15$, and $r = 0.3$. We see that the value of $\theta_{jl}^{(r)}$ is close to 90° for some values of ϕ. From the results in the case of sinusoidal forcing, we know that when the wave vectors of two standing waves are separated by an angle of $\theta_{jl}^{(r)}$, the pattern is strongly suppressed. Two waves of wave vectors separated by this angle will excite a linearly stable mode with an amplitude inversely proportional to the damping coefficient. Energy is then dissipated by the stable mode, and hence the two original waves are effectively damped as compared to other unstable modes that do not satisfy the triad resonance condition. Thus, without further calculations one
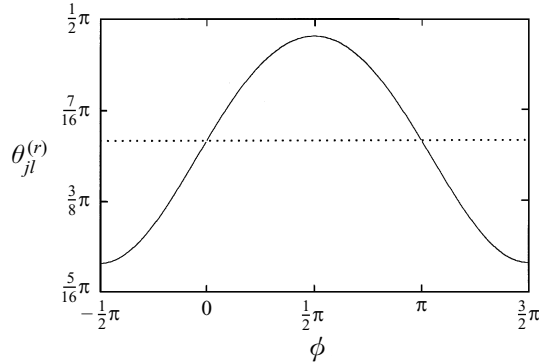
FIGURE 2. Modified triad resonant condition, $\theta_{jl}^{(r)}$, as a function of the phase difference ϕ, for the subharmonic response in two-frequency Faraday waves of frequency ratio 1:2 with $\Gamma_0 = 1$, $\gamma = 0.15$, and $r = 0.3$. The dashed line corresponds to the value of $\theta_{jl}^{(r)}$ for purely capillary waves in the case of sinusoidal forcing.

already can conclude that square patterns are not favoured when the phase difference ϕ is close to $\pi/2$ (or φ close to 0 in Müller's notation) for this set of parameters.

At $O(\varepsilon^{3/2})$, the calculation is again similar to the case of single-frequency forcing. The solvability condition gives the following standing wave amplitude equations:

$$\frac{1}{\gamma}\frac{\partial A_j}{\partial T} = A_j - \left[g(1)|A_j|^2 + \sum_{l=1(l\neq j)}^{N} g(c_{jl})|A_l|^2 \right] A_j, \tag{3.29}$$

where $j = 1, 2, \cdots, N$,

$$g(1) = \frac{28 + 9\Gamma_0 + (12 + 9\Gamma_0)\kappa\cos\phi}{64} + 2\alpha_{jj} + \frac{3(1 + \kappa\cos\phi)}{8}\beta_{jj} - \tfrac{1}{2}\delta_{jj}, \tag{3.30}$$

and

$$\begin{aligned}
g(c_{jl}) = {}& \frac{3\Gamma_0(1+\kappa\cos\phi)}{32}\left(1+2c_{jl}^2\right) + \frac{7+3\kappa\cos\phi}{8}\left(3 - [2(1+c_{jl})]^{1/2} - [2(1-c_{jl})]^{1/2}\right) \\
& + \left(1 + c_{jl} - [2(1+c_{jl})]^{1/2}\right)\left(\frac{1+\kappa\cos\phi}{4}w_{jl} - v_{jl}\right) \\
& + \left(1 - c_{jl} - [2(1-c_{jl})]^{1/2}\right)\left(\frac{1+\kappa\cos\phi}{4}\bar{w}_{jl} - \bar{v}_{jl}\right) \\
& + (1 + c_{jl})\left(2\alpha_{jl} + \frac{3(1+\kappa\cos\phi)}{8}\beta_{jl} - \tfrac{1}{2}\delta_{jl}\right) \\
& + (1 - c_{jl})\left(2\bar{\alpha}_{jl} + \frac{3(1+\kappa\cos\phi)}{8}\bar{\beta}_{jl} - \tfrac{1}{2}\bar{\delta}_{jl}\right).
\end{aligned} \tag{3.31}$$

When $\kappa = 0$, (3.29) reduces to the standing wave amplitude equation for sinusoidal forcing as expected (Zhang & Viñals 1997).

In contrast to single-frequency forced Faraday waves, we note that $g(1) < 0$ for some ranges of parameter values in this two-frequency case. When $g(1) < 0$, the amplitude A_j would increase without limit. Therefore higher-order terms (at least of fifth order) will be required in the SWAE to saturate the amplitude. The regions where $g(1) < 0$ for particular sets of parameters are shown black in figure 5. The steady state of parametric surface waves in parameter regions such that $g(1) < 0$

cannot be determined from the SWAEs, (3.29). Analytical calculations of the relevant higher-order terms in this case are algebraically much more complicated than the calculations presented here, and we have not done such calculations. We shall restrict ourselves to the parameter range that gives a positive $g(1)$ in further analysis of this section.

When $g(1) > 0$, we can rescale the amplitude A_j in (3.29) as $\tilde{A}_j = (g(1))^{1/2}A_j$. We have the following standing wave amplitude equation for the scaled amplitude:

$$\frac{1}{\gamma}\frac{\partial \tilde{A}_j}{\partial T} = \tilde{A}_j - \left[|\tilde{A}_j|^2 + \sum_{l=1(l\neq j)}^{N} \tilde{g}(c_{jl})|\tilde{A}_l|^2\right]\tilde{A}_j, \qquad (3.32)$$

where $\tilde{g}(c_{jl}) = g(c_{jl})/g(1)$. Note that $\tilde{g}(c_{jl} \to \pm 1) = 2$.

The scaled nonlinear interaction coefficient $g(c_{jl})$ (we have suppressed the tilde since we will only refer to the scaled nonlinear coefficient in what follows) for the regions with a positive $g(1)$ depends strongly on the phase difference ϕ. This is due to the effect of the modified triad resonant condition (see figure 2), as well as other effects, such as the dependence of the surface wave amplitude at the modified triad resonance on ϕ. As an example, figure 3(a) shows the scaled coefficient $g(c_{jl})$ as a function of c_{jl} for purely capillary waves with $\gamma = 0.1$ and $r = 0.25$. The general trend in these curves can be understood from the different triad resonant condition for different values of ϕ. As ϕ decreases from $3\pi/2$ to $\pi/2$, the angle $\theta_{jl}^{(r)}$ (recall that $c_{jl} = \cos(\theta_{jl})$) at the triad resonance increases to a value close to $\pi/2$ (see figure 2), and therefore the value of $g(c_{jl})$ changes from a minimum (< 1) to a local maximum (> 1). This change in $g(c_{jl})$ makes a pattern of square symmetry unstable for ϕ close to $\pi/2$ (since $g(0) > 1$). By increasing the value of r in figure 3(b), the amplitude of the smaller forcing component $(\kappa \sin(4t + \phi))$ decreases, and therefore the changes in $g(c_{jl})$ for different values of ϕ are smaller. We note that with the damping parameters used in figure 3, surface waves may have a synchronous (harmonic) response to the driving force, i.e. below the bicritical line in figure 1 for some values of the phase difference ϕ. In that case, the above results for $g(c_{jl})$ become irrelevant for these values of ϕ.

For larger values of the damping parameter γ, triad resonant interactions are more strongly damped, as is the case for single-frequency forcing. However, the situation is more complicated here since the modified triad resonant condition depends on γ (actually it depends on the driving amplitude f, which is approximately equal to γ at onset). For example, larger values of γ can make the angle $\theta_{jl}^{(r)}$ at the triad resonance closer to $\pi/2$. Figure 4 shows the function $g(c_{jl})$ for the same values of parameters as in figure 3 except the value of γ is raised to $\gamma = 0.15$.

3.2. *Pattern selection near onset*

A qualitative analysis of pattern selection for the two-frequency case has already been advanced by Müller (1993), based on general symmetry considerations and a typical shape of the nonlinear coupling function $g(c_{jl})$. The derivation of this function given in the previous subsection allows us to obtain quantitative predictions for the regions in parameter space in which patterns of a given symmetry minimize the appropriate Lyapunov function for this problem. Since (3.32) is of gradient form $(1/\gamma)\partial_T A_j = -\partial\mathscr{F}/\partial A_j^*$, a Lyapunov function $\mathscr{F}$ can be defined as

$$\mathscr{F} = -\sum_{j=1}^{N}|A_j|^2 + \frac{1}{2}\sum_{j=1}^{N}|A_j|^2\left(|A_j|^2 + \sum_{l=1(l\neq j)}^{N} g(c_{jl})|A_l|^2\right). \qquad (3.33)$$
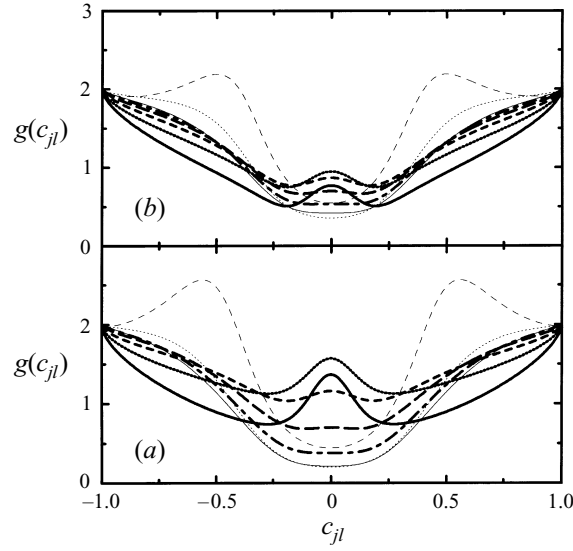
FIGURE 3. Nonlinear coefficient $g(c_{jl})$ of the SWAEs for two-frequency driven Faraday waves for purely capillary waves with damping parameter $\gamma = 0.1$ and the relative amplitude $r = 0.25$ in (*a*), $r = 0.35$ in (*b*). The phase difference $\phi = \pi/2$ for the thick solid curves, $\phi = 0.6\pi$ for the thick dotted curves, $\phi = 0.7\pi$ for the thick dashed curves, $\phi = 0.8\pi$ for the thick long-dashed curves, $\phi = 0.9\pi$ for the thick dot-dashed curves, $\phi = \pi$ for the thin solid curves, $\phi = 1.3\pi$ for the thin dotted curves, and $\phi = 3\pi/2$ for the thin dashed curves.
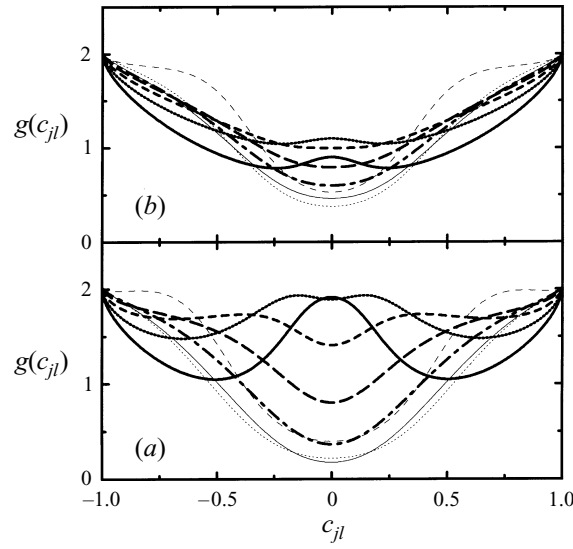

FIGURE 4. As figure 3 but with damping parameter $\gamma = 0.15$.

Since

$$\frac{\mathrm{d}\mathscr{F}}{\mathrm{d}T} = \sum_{j=1}^{N} \left(\frac{\partial \mathscr{F}}{\partial A_j} \partial_T A_j + \frac{\partial \mathscr{F}}{\partial A_j^*} \partial_T A_j^* \right) = -\frac{2}{\gamma} \sum_{j=1}^{N} |\partial_T A_j|^2 \leqslant 0, \qquad (3.34)$$

the only possible limiting cases of such a dissipative system, in the limit $T \to \infty$, are stationary states for the amplitudes A_j. Only the states which correspond to local minima of the Lyapunov function are linearly stable.

Apart from the trivial solution of $A_j = 0$ for $j = 1, \cdots, N$, (3.32) has a family of stationary solutions differing in the total number of standing waves N for which $A_j \neq 0$. By considering the case in which the magnitudes of all standing waves are the same, i.e. $|A_j| = |A|$, (3.32) has the following solutions:

$$|A_j| = |A| = \left(1 + \sum_{l=1(l \neq j)}^{N} g(c_{jl})\right)^{-1/2}. \tag{3.35}$$

The values of the Lyapunov function for these solutions are

$$\mathscr{F} = -\frac{N}{2}|A|^2 = -\frac{N/2}{1 + \sum\limits_{l=1(l \neq j)}^{N} g(c_{jl})}. \tag{3.36}$$

We shall only consider pattern structures for which the angle between any two adjacent wave vectors $\boldsymbol{k}_j$ and $\boldsymbol{k}_{j+1}$ is the same and is π/N (regular pattern). We summarize our results concerning regular patterns in figure 5. Note that our results only apply to the subharmonic response to the driving force, which corresponds to the side of bicritical line with smaller amplitude ratio r. Different regions are labelled by the pattern structure that has the lowest value of the Lyapunov function $\mathscr{F}_N$ except the region shown in black, in which the self-interaction coefficient $g(1)$ is negative. Figure 5(a) uses all the appropriate fluid and forcing parameters from Müller's experiment (Müller 1993). As shown in figure 5(a), hexagonal or triangular patterns have the lowest value of Lyapunov function in a region around $\phi = \pi/2$ and close to the bicritical line, while square pattern is stable near the bicritical line and around $\phi = 3\pi/2$ (or $-\pi/2$). This result is in qualitative agreement with Müller's experiment although our theory predicts a smaller stable hexagonal/triangular region for this set of parameter values. In a region close to the bicritical line and with $0 \leqslant \phi \leqslant \pi/2$, differences in the values of the Lyapunov function for different patterns become smaller, and most stable patterns of different symmetries (including quasi-crystalline ones) correspond to neighbouring smaller parameter regions. It is possible that the preferred pattern may not be selected due to such small differences in Lyapunov function for patterns of different symmetries, or there is no selection at all. This result is in partial agreement with Müller's experiment, where he found disordered patterns in a parameter region overlapping with the above-mentioned region.

Figure 5(b–d) uses the same parameter values except the fluid viscosity which is changed from $v = 0.20$ cm^{-2} s^{-1} to 0.15 cm^{-2} s^{-1}, 0.10 cm^{-2} s^{-1}, and 0.05 cm^{-2} s^{-1} respectively. We note that as v decreases (smaller viscous damping), the hexagonal/triangular region becomes larger and the centre of this region is also shifted towards a larger value of ϕ. For $v = 0.05$ cm^2 s^{-1}, the hexagonal/triangular region reaches larger values of $r > 0.60$. Currently there are no experimental results known to us that can be used to test our predictions as the damping parameter varies.

4. Discussion and summary

We comment further on the approximations used to obtain our main results presented in figure 5. In the quasi-potential approximation, terms of the order of
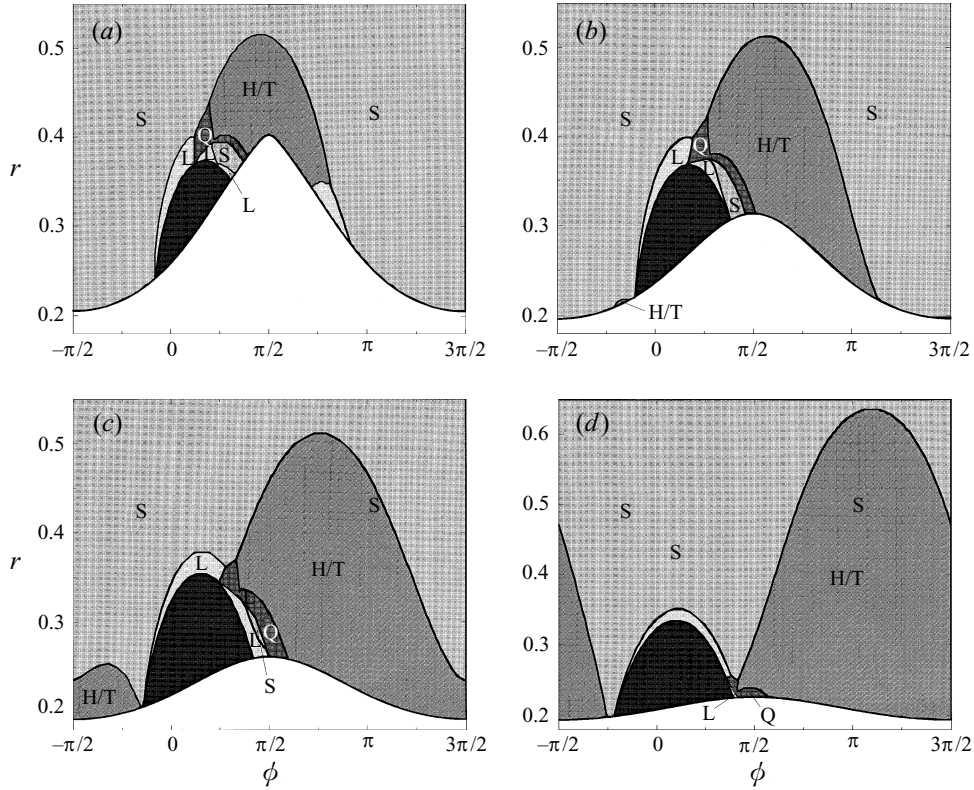
FIGURE 5. Regions labelled by the pattern structure that has the lowest value of the Lyapunov function: L – lines, S – square, H/T – hexagon/triangle, and Q – quasi-crystalline patterns (8-fold, 10-fold, 12-fold, ...). The black region indicates where the self-interaction coefficient $g(1)$ is negative. (a) Calculated using parameters of Müller's experiment: $\rho = 0.95$ g cm^{-3}, $\Gamma = 20.6$ dyn cm^{-1}, $v = 0.20$ cm^2 s^{-1}, $\omega_0/2\pi = 27.9$ Hz, $2\pi/k_{12s} = 0.72$ cm, and $2\pi/k_{12h} = 17.0$ cm. (b–d) Calculated using the same values of ρ, Γ, ω_0, k_{12s}, and k_{12h} as (a) but $v = 0.15$ cm^2 s^{-1}, $v = 0.1$ cm^2 s^{-1}, and $v = 0.05$ cm^2 s^{-1} respectively. Note the different r scale used for (d).

$\gamma^{3/2}$ or higher have been neglected. Consistent with that, we use approximate linear solutions, correct up to order f or γ (the perturbation expansion for the linear solutions) in deriving the SWAEs, (3.29). On the other hand, we included terms of the order of f^2, $f\gamma$, or γ^2 in the linear stability analysis to obtain the bicritical line. We considered these terms because of the large coefficients for such terms in the perturbation expansion for the bicritical line in order to compare our results with Müller's experiment which used relatively large values of γ (especially for the case of harmonic response $\gamma_h = 0.33$). A fully consistent calculation correct up to the order of γ^2 will be much more difficult. Based on the qualitative agreement of the bicritical line we obtained with experiments, we expect that a fully consistent calculation would change our results quantitatively, but not qualitatively.

In summary, analytical results for bicritical lines $r_b(\phi)$ are obtained by using a multiscale perturbation expansion. The results for $r_b(\phi)$ for frequency ratio 1/2 agree qualitatively with Müller's experimental results. We also derive the SWAEs for frequency ratio 1/2 (for the case of subharmonic response). We found that the triad resonance condition is modified due the presence of the second frequency component. For certain values of the relative phase difference between the two forcing components,

we found that $\theta_{jl}^{(r)}$ becomes close to 90°. As a result, square patterns become unstable in this parameter region. Even though quadratic terms are prohibited for subharmonic responses, hexagonal or triangular patterns can be stabilized with the presence of the second frequency component, which is in agreement with experiments. We also studied pattern selection for different values of the damping parameters, and found that hexagonal/triangular patterns are stabilized in a larger region for smaller values of the damping parameter. This is a prediction that awaits experimental verification.

REFERENCES

BOSCH, E. & WATER, W. VAN DE 1993 *Phys. Rev. Lett.* **70**, 3420.

CHRISTIANSEN, B., ALSTRØM, P. & LEVINSEN, M. T. 1992 *Phys. Rev. Lett.* **68**, 2157.

CILIBERTO, S., DOUADY, S. & FAUVE, S. 1991 *Europhys. Lett.* **15**, 23.

CROSS, M. C. & HOHENBERG, P. C. 1993 *Rev. Mod. Phys.* **65**, 851.

EDWARDS, W. S. & FAUVE, S. 1992 *C. R. Acad. Sci. Paris* II **315**, 417.

EDWARDS, W. S. & FAUVE, S. 1993 *Phys. Rev.* E **47**, 123.

EDWARDS, W. S. & FAUVE, S. 1994 *J. Fluid Mech.* **278**, 123.

EZERSKII, A., RABINOVICH, M., REUTOV, V. & STAROBINETS, I. 1986 *Zh. Eksp. Tero. Fiz.* **91**, 2070 (transl. 1986 *Sov. Phys. JETP* **64**, 1228).

KUDROLLI, A. & GOLLUB, J. P. 1996 *Physica* D **97**, 133.

LANDAU, L. D. & LIFSHITZ, E. M. 1976 *Fluid Mechanics*, 3rd edn. Pergamon.

LANG, R. J. 1962 *J. Acoust. Soc. Am.* **34**, 6.

MILES, J. W. & HENDERSON, D. 1990 *Ann. Rev. Fluid Mech.* **22**, 143.

MÜLLER, H. 1993 *Phys. Rev. Lett.* **71**, 3287.

TUFILLARO, N. B. & GOLLUB, J. P. 1989 *Phys. Rev. Lett.* **62**, 422.

ZHANG, W. & VIÑALS, J. 1996 *Phys. Rev.* E **53**, R4283.

ZHANG, W. & VIÑALS, J. 1997 *J. Fluid Mech.* **336**, 301.